MOV10L1 is necessary for protection of spermatocytes against retrotransposons by Piwi-interacting RNAs

Robert J. A. Frost[a], F. Kent Hamra[b], James A. Richardson[a,c], Xiaoxia Qi[a], Rhonda Bassel-Duby[a], and Eric N. Olson[a,1]

[a]Department of Molecular Biology, [b]Cecil H. and Ida Green Center for Reproductive Biology Sciences, and [c]Department of Pathology, University of Texas Southwestern Medical Center, Dallas, TX 75390-9148

Piwi-interacting RNAs (piRNAs) comprise a broad class of small noncoding RNAs that function as an endogenous defense system against transposable elements. Here we show that the putative DExD-box helicase MOV10-like-1 (MOV10L1) is essential for silencing retrotransposons in the mouse male germline. *Mov10l1* is specifically expressed in germ cells with increasing expression from gonocytes/type A spermatogonia to pachytene spermatocytes. Primary spermatocytes of *Mov10l1*−/− mice show activation of LTR and LINE-1 retrotransposons, followed by cell death, causing male infertility and a complete block of spermatogenesis at early prophase of meiosis I. Despite the early expression of *Mov10l1*, germline stem cell maintenance appears unaffected in *Mov10l1*−/− mice. MOV10L1 interacts with the Piwi proteins MILI and MIWI. MOV10L1 also interacts with heat shock 70-kDa protein 2 (HSPA2), a testis-enriched chaperone expressed in pachytene spermatocytes and also essential for male fertility. These studies reveal a crucial role of MOV10L1 in male fertility and piRNA-directed retrotransposon silencing in male germ cells and suggest that MOV10L1 functions as a key component of a safeguard mechanism for the genetic information in male germ cells of mammals.

RNA helicase | Armitage | meiosis

Approximately 45% of the human genome is derived from transposable elements, the majority of which originate from retrotransposons (1). Retrotransposons drive their own genomic replication via an RNA intermediate that is reverse transcribed before its integration into the genome. Retrotransposons can be categorized into long-terminal repeat (LTR) retrotransposons (~8.3% of the human genome) and non-LTR retrotransposons such as LINE-1 (long interspersed element 1; ~16.9% of the human genome), and Alu elements (~10.6% of the human genome) (1). LTRs are retrotransposon sequences of 300–1,000 bp that are directly repeated at the 5′ and 3′ ends. The canonical LINE-1 retrotransposon is 6 kb long and comprises a 5′ UTR with an internal RNA polymerase II promoter, two ORFs encoding for an RNA-binding protein (ORF1) and a protein with endonuclease and reverse-transcriptase activity (ORF2), and a 3′ UTR with a polyadenylation signal (2). Due to truncations and mutations, less than 100 and 3,000 of the estimated >500,000 copies of LINE-1 elements are believed to be still functional in the human and mouse genomes, respectively (3, 4). Retrotransposon replication likely has had a major impact on the evolution of the human genome (1); however, uncontrolled retrotransposon activity results in genomic instability and cell death due to insertional mutagenesis. In somatic cells, retrotransposons are suppressed by DNA methylation, but they are not suppressed in male germ cells when, during a short period of intensive epigenetic reprogramming, DNA methylation is temporarily lost (5).

Male germ cells undergo a dramatic developmental process called spermatogenesis. In mice, spermatogenesis can be divided into 12 stages, each of which consists of a specific complement of male germ cells (6). Initiated on day 3 after birth, a series of mitoses of germline stem cells, a subset of type A spermatogonia, gives rise to type B spermatogonia that appear at day 8 after birth. Leptotene, zygotene, and pachytene spermatocytes follow

on days 10, 12, and 14, respectively. Meiosis of those primary spermatocytes leads to the production of haploid round spermatids that subsequently transform via elongating spermatids into mature sperm.

Recently, an endogenous Piwi-interacting RNA (piRNA)-based defense system that silences retrotransposon activity in germ cells through both transcriptional and posttranscriptional mechanisms was discovered (7). Transcriptional silencing mechanisms include piRNA-mediated DNA remethylation of retrotransposon regions (5). piRNAs are a multitudinous class of ~26- to 31-nucleotide RNA molecules that are processed by a Dicer-independent mechanism from long, single-stranded precursor transcripts that often encode several piRNAs (7). Germ cells in mice express two types of piRNAs: (*i*) a small fraction of piRNAs derived from repetitive genomic regions expressed during mouse embryogenesis and (*ii*) a larger fraction of piRNAs derived from nonrepetitive regions that starts to become expressed during the pachytene stage of meiosis (pachytene piRNAs) (7). Pachytene piRNAs interact with MIWI (mouse PIWI) and MILI (MIWI-like), two of the three murine Piwi proteins, a subfamily of the Argonaute-proteins (8). MIWI2, the third murine Piwi protein, is also expressed specifically in the germline before birth.

We discovered a putative DExD-box helicase (called CHAMP; cardiac helicase activated by MEF2C protein), encoded by differently sized transcripts in heart (exons 15–26) and testis (exons 1–26) (9). The testis-specific isoform has also been referred to as MOV10-like-1 (MOV10L1), on the basis of its extensive homology to Moloney leukemia virus 10 (MOV10), which was shown to interact with argonaute 1 and 2 in HeLa cells (10). The *Drosophila* homolog of CHAMP/MOV10L1/MOV10, known as Armitage, is necessary for piRNA processing in germ cells of *Drosophila* (11, 12).

To investigate the function of MOV10L1 in mammals, we generated mice harboring a global deletion of the *Mov10l1* gene. These mice were viable and healthy, but male *Mov10l1*-null (*Mov10l1*−/−) mice were infertile due to apoptotic loss of early pachytene spermatocytes, which was preceded by retrotransposon activation. Our results identify MOV10L1 as an interacting partner of MILI and MIWI, and we conclude that this interaction is a key conserved feature in safeguarding DNA of male germ cells against retrotransposons.

Results and Discussion

Mov10l1 Is Predominantly Expressed in Pachytene Spermatocytes.
Recent studies show that the function of PIWI in germ cells of *Drosophila* depends on the putative RNA helicase Armitage (11, 12). Mice and humans have two genes that are predicted to be homologous to *Armitage*, *Mov10*, and *Mov10l1*. To determine the expression patterns of these putative *Armitage* homologs in mouse

---

testis, we analyzed expression of *Mov10* and *Mov10l1* postnatally during development of the first spermatogenic waves (Fig. 1*A*). On the basis of microarray data that we had previously deposited at the Gene Omnibus database, expression of *Mov10* was low and did not change significantly between postnatal days (P) 1 and 29. In contrast, by P14, the relative abundance of *Mov10l1* had increased sixfold to peak with the rise of pachytene spermatocytes. After P21, the abundance of *Mov10l1* transcripts steadily declined, coincident with the emergence of the first generations of round and elongating spermatids. This expression pattern mirrored that of *Mili*, one of the three murine Piwi genes that are necessary for piRNA synthesis and function. To determine whether *Mov10l1* expression in testis was restricted to spermatogonic cells, we analyzed spermatogonic and somatic cell fractions from mouse testis. *Mov10l1* transcripts were abundant in spermatogenic cells, but absent in tubular or interstitial somatic cells (Fig. 1*B*).

To verify that *Mov10l1* expression is restricted to the germline, we performed radioactive in situ hybridization on testis sections at embryonic day 18 (E18), at P15, and at 7 wk of age. Two separate probes directed against the sense strand of the C-terminal coding region of *Mov10l1* and the 3′ UTR of *Mov10l1*, respectively, showed an identical expression pattern of *Mov10l1*. At E18, *Mov10l1* was specifically expressed within the testis in gonocytes, not in tubular or interstitial somatic cells (Fig. 1*C*, *Upper*). In juvenile (P15) and adult mice (7 wk old), *Mov10l1* expression was most abundant in pachytene spermatocytes and absent in more mature spermatogenic cells and in somatic cells (Fig. 1*C*, *Lower*). Notably, exposure of the embryonic tissue was 3 wk, whereas exposure of juvenile and adult testis sections was only 1 wk, resulting in an overestimation of the expression of *Mov10l1* in embryonic compared with adult testis. A negative control probe directed against the antisense strand of the C-terminal coding region of *Mov10l1* showed no specific signal.

In addition to full-length *Mov10l1*, two additional *Mov10l1* transcripts, *Champ* and *Csm* (cardiac specific transcript of *Mov10l1*), were described previously as smaller transcripts (9, 13, 14) (Fig. S1*A*). EST databases also suggested an additional transcript starting at exon 20 (*E20-SV*). We determined expression of all four putative *Mov10l1* transcripts in heart and testis by real-time PCR (Fig. S1*B*). We found that, in addition to the very weak expression of the putative exon 20 transcript, adult testis expressed only full-length *Mov10l1* and adult heart predominantly the *Csm* transcript, suggesting that

the *Mov10l1* signal, which was detected by microarray and in situ hybridization analysis of testis tissue, represents full-length *Mov10l1*.

Global Deletion of *Mov10l1* Blocks Spermatogenesis During Meiosis I.

To assess the function of *Mov10l1* in vivo, we generated mice lacking a functional *Mov10l1* gene. Because it has been shown that the helicase domain residing in exon 20 is necessary for an antiproliferative function of CHAMP in vitro (15), and because both CHAMP and MOV10L1 share this domain, we chose to flank exon 20 of the *Mov10l1* gene with *lox*P sites (Fig. 2*A* and Fig. S2*A*). We generated targeted embryonic stem cells that carried the floxed exon 20 of *Mov10l1* as shown by Southern blot analysis (Fig. S2*B*) and injected those mutant cells into blastocysts to obtain chimeric mice. For generation of *Mov10l1* knockout mice, we crossed germline-transmitted mice to transgenic mice that globally expressed *Cre recombinase* under the control of the CAG promoter (CAG-Cre). The absence of *Mov10l1* mRNA starting from exon 20 was confirmed by PCR (Fig. S2*C*). Furthermore, we did not observe any specific *Mov10l1* signal in testis sections of *Mov10l1*$^{-/-}$ mice by radioactive in situ hybridization (Fig. S2*D*). Deletion of *Mov10l1* did not result in compensatory expression of *Mov10* (Fig. S2*E*).

Mov10l1$^{-/-}$ mice were obtained at predicted Mendelian ratios from heterozygous intercrosses. *Mov10l1*$^{-/-}$ mice appeared healthy, even though they also lacked expression of CHAMP and CSM in the heart; however, male *Mov10l1*$^{-/-}$ mice were infertile.

It was recently suggested that reduced *Mov10l1* levels were at least partially responsible for accelerated ovarian aging and follicle depletion in mice that lack the transcriptional regulator TAF4B (16). However, in contrast to this proposal, female *Mov10l1*$^{-/-}$ mice appeared to have normal and sustained fertility (9 ± 1.1 pups per litter; $n = 10$ litters), and we assume therefore that reduced *Mov10l1* expression in TAF4B$^{-/-}$ mice is a marker rather than a cause for accelerated ovarian aging. The lack of an obvious phenotype of *Mov10l1*$^{-/-}$ mice in ovaries is surprising given the fact that ovaries also express piRNAs. However, other mouse models with genetic deletions of proteins involved in piRNA processing/ function also show solely male infertility (17–21).

Testes of 3-mo-old *Mov10l1*$^{-/-}$ mice were significantly smaller than testes of *Mov10l1*$^{+/-}$ or *Mov10l1*$^{+/+}$ littermates (Fig. 2*B*). This phenotype was observed with 100% penetrance, emphasizing
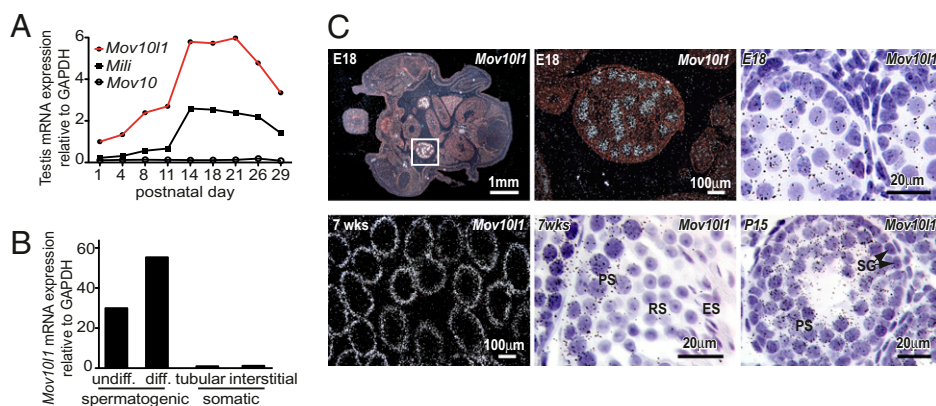

Fig. 1. *Mov10l1* is specifically expressed in spermatocytes within the testis. (*A*) Expression of *Mov10l1*, *Mov10*, and *Mili* mRNA in testes of C57BL/6 mice during postnatal development (GEO Series GES640). (*B*) *Mov10l1* mRNA expression in fractions of undifferentiated (undiff.) spermatogonia and spermatocytes (diff.) compared with tubular and interstitial somatic testis cells isolated from testes of 19-d-old C57BL/6 mice (GEO series GES829). (*C*) Detection of *Mov10l1* in embryonic (*Upper*) and juvenile/adult (*Lower*) testes by radioactive in situ hybridization with a probe directed against the C-terminal region of *Mov10l1*; exposure was 3 wk for embryonic and 1 week for postnatal tissue. (*Upper Left*) A dark-field image of a transverse section through the lower abdomen of an embryonic day 18 (E18) mouse. (*Upper Center*) An enlargement of *Upper Left* showing *Mov10l1* mRNA as bright white dots in testis. (*Upper Right*) A high-magnification bright-field image of a seminiferous tubule depicting *Mov10l1* as black silver grains localized specifically in gonocytes. (*Lower*) Detection of *Mov10l1* in 7-wk-old adult (*Lower Left*, dark-field; *Lower Center*, bright-field) and in P15 juvenile (*Lower Right*) mouse testis. PS, pachytene spermatocytes; RS, round spermatids; ES, elongating spermatids; SG, spermatogonia.
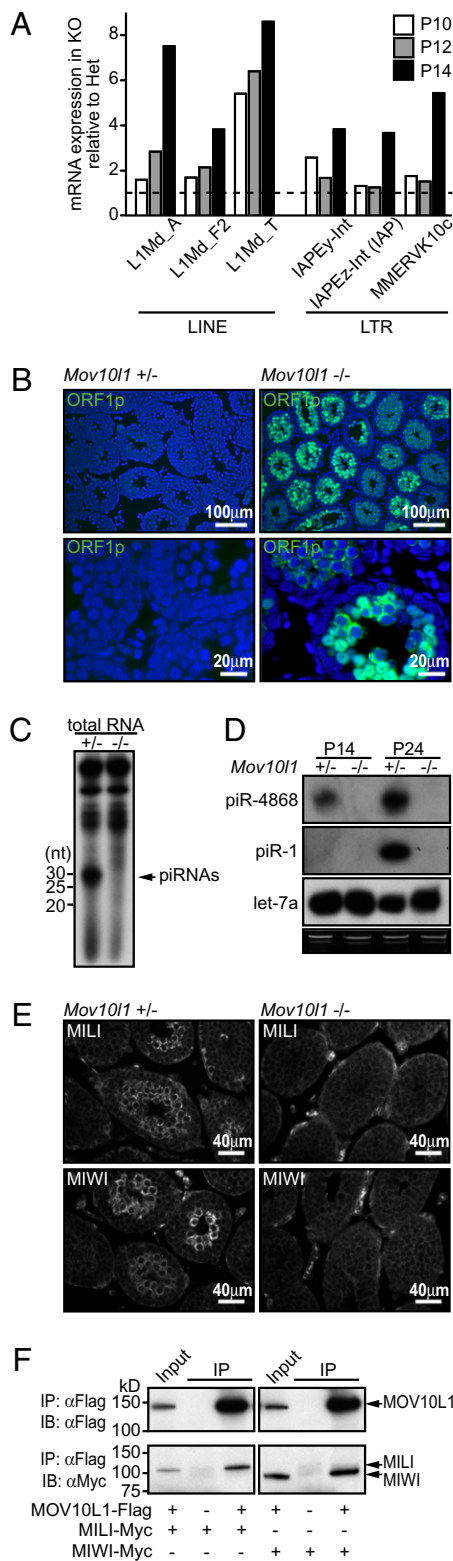
Fig. 2. *Mov10l1⁻/⁻* mice have a reduced testis size secondary to a lack of spermatids. (*A*) Scheme of the predicted MOV10L1 domains. For generation of *Mov10l1⁻/⁻* mice, the exon encoding the putative helicase domain (red) was flanked by *LoxP* sites, and global deletion of *Mov10l1* was then achieved by breeding *Mov10l1⁺/ᶠˡ* mice to CAG-*Cre* transgenic mice. (*B*) *Mov10l1⁻/⁻* mice showed reduced testis size compared with *Mov10l1⁺/⁻* and *Mov10l1⁺/⁺* mice. (*Left*) Testes of 3-mo-old mice from the same litter. (*Right*) Testis weight of *Mov10l1⁺/⁻* and *Mov10l1⁻/⁻* mice. Each time point represents the mean of two to six testes. (*C*) Representative hematoxylin and eosin staining of transverse sections through testes of 3-mo-old wild-type versus *Mov10l1⁻/⁻* mice. (*Lower*) An enlargement of the regions indicated by the black frame in the *Upper*. ES, elongating spermatids; RS, round spermatids; PS, pachytene spermatocytes; DS, degenerating spermatocytes with condensed nuclei.

the crucial importance of *Mov10l1* even in a mixed genetic background. We determined testis weight at different ages and found that developmental increase in testis size was initially normal in *Mov10l1⁻/⁻* mice; however, growth was markedly slowed at postnatal week 3 and arrested shortly thereafter (Fig. 2*B* and Fig. S2*F*). The overall testis architecture seemed to be normal; however, individual seminiferous tubules of *Mov10l1⁻/⁻* testes were significantly smaller than those of wild-type testes, explaining the reduced size of testes in *Mov10l1⁻/⁻* mice (Fig. 2*C*). Seminiferous tubules of testes from adult *Mov10l1⁻/⁻* mice contained Sertoli cells and early stages of spermatogonic cells; however, many pachytene-like spermatocytes appeared to have degenerating nuclei and round spermatids, and elongating spermatids were missing completely (Fig. 2*C, Lower*). Furthermore, epididymides of adult *Mov10l1⁻/⁻* mice were free of any mature sperm (Fig. 3 *A* and *B*).

To determine the time of onset of abnormalities in *Mov10l1⁻/⁻* testis, we examined testis sections during development of the first generations of type B spermatogonia (P8), leptotene spermatocytes (P10), and pachytene spermatocytes (P14 and P15) (Fig. S3 *A–H*). Cross-sections of *Mov10l1⁻/⁻* and *Mov10l1⁺/⁻* testes appeared similar until P14. However, beginning at P15, seminiferous tubules of *Mov10⁻/⁻* mice demonstrated degenerating cells with hyperchromatic nuclei (Fig. S3 *G* and *H*). TUNEL staining of the same sections to determine abundance of apoptotic cells showed similar numbers of apoptotic cells in *Mov10l1⁺/⁻* and *Mov10l1⁻/⁻* mice at P8, P10, and P14. Starting at P15, some seminiferous tubules of

Mov10l1⁻/⁻ mice showed massive TUNEL staining of the most mature spermatocytes (Fig. 3 *C* and *D*). Interestingly, in contrast to the specific staining of nuclei in apoptotic cells of control animals, TUNEL staining in strongly affected tubules of *Mov10l1⁻/⁻* mice seemed to start in the cytoplasm (arrowhead in Fig. 3*D*) and was

Fig. 3. Infertility of *Mov10l1⁻/⁻* mice due to cell death of early pachytene spermatocytes. (*A* and *B*) Hematoxylin and eosin (H&E)-stained sections of epididymides of 3-mo-old mice. Sperm were absent in epididymides of *Mov10l1⁻/⁻* mice. (*C* and *D*) TUNEL staining of sections from testis of P15 *Mov10l1⁺/⁻* and *Mov10l1⁻/⁻* mice, respectively. (*Left*) Red channel with the apoptotic nuclei. (*Right*) Overlay with DAPI-stained nuclei (blue). (*E–H*) Confocal microscopy images of immunofluorescent staining of testis sections from P14-old mice for SCP1 (synaptonemal complex protein 1) and SCP3, respectively; counterstaining of nuclei with DAPI (blue) in *G* and *H*. (*I* and *J*) H&E staining of transverse sections of 9.5-mo-old mice; seminiferous tubules *Mov10l1⁻/⁻* mice still contained many spermatocytes and degenerating cells (arrowhead in *J*). (*K* and *L*) PZLF staining of tubules isolated from testes of 6-mo-old wild-type and *Mov10l1⁻/⁻* mice, respectively.

seen later in nuclei. At 5 wk of age, the majority of seminiferous tubules in *Mov10l1*$^{-/-}$ mice showed an abundance of TUNEL-positive cells (Fig. S3 *K–N*).

To further define the meiotic defects in *Mov10l1*$^{-/-}$ testes, we analyzed the assembly of the synaptonemal complex (SC) by immunostaining. Expression of SCP (synaptonemal complex protein) 1, which is a major component of the transverse filaments of the SC and is first expressed in zygotene spermatocytes, was absent in *Mov10l1*$^{-/-}$ testes (Fig. 3 *E* and *F*). Expression of SCP3, which is a component of the axial element of the SC and is expressed from leptotene spermatocytes to late meiotic cells, appeared in some seminiferous tubules of *Mov10l1*$^{-/-}$ mice similarly to the tubules of wild-type mice (Fig. 3 *G* and *H*). However, in contrast to wild-type mice, the majority of seminiferous tubules of *Mov10l1*$^{-/-}$ mice showed relatively strong, abnormal staining of chromosomal structures (Fig. 3*H*, right tubule), which might indicate failure of the SC to assemble properly in more differentiated germ cells. Thus, disruption of *Mov10l1* causes meiotic blockade before the pachytene stage.

Because *Mov10l1* mRNA is already expressed in gonocytes (Fig. 1*C*, *Upper*) and because deletion of several PIWI-complex proteins such as MILI, MIWI2, and GASZ causes Sertoli-cell-only tubules due to a progressive loss of undifferentiated germ cells with age (19, 20, 22), we also performed histological analysis of testes from 9.5-mo-old *Mov10l1*$^{-/-}$ mice. Seminiferous tubules of these old *Mov10l1*$^{-/-}$ mice still showed a high cell turnover with many mitotic and degenerating cells, suggesting that MOV10L1 is not required for maintenance of germline stem cells (Fig. 3 *I* and *J*). Furthermore, staining of PLZF (promyelocytic leukemia zinc finger), a marker for undifferentiated germ cells (23), in tubules of 6-mo-old mice, showed that, even though isolated tubules of *Mov10l1*$^{-/-}$ mice were significantly thinner than wild-type tubules, they nevertheless contained numerous undifferentiated spermatogonia (Fig. 3 *K* and *L*).

Mov10l1 Is Necessary for piRNA-Dependent Repression of Retrotransposons. Massive cell death, which resulted in the lack of round and elongating spermatocytes in *Mov10l1*$^{-/-}$ mice, started at P15. To investigate the mechanism for cell death in *Mov10l1*$^{-/-}$ mice, we compared the gene expression patterns of testes from *Mov10l1*$^{+/-}$ and *Mov10l1*$^{-/-}$ mice at 10, 12, and 14 d of age. Genes up-regulated more than twofold or down-regulated >50% at P14 in *Mov10l1*$^{-/-}$ mice compared with *Mov10l1*$^{+/-}$ mice are presented in Dataset S1 and Dataset S2. At P12, gene expression was similar in *Mov10l1*$^{+/-}$ and *Mov10l1*$^{-/-}$ mice. However, many genes that were up-regulated between P12 and P14 in *Mov10l1*$^{+/-}$ mice failed to be up-regulated in *Mov10l1*$^{-/-}$ mice. These findings suggest that *Mov10l1*$^{-/-}$ mice have a block of spermatogenesis starting at the transition from zygotene to pachytene spermatocytes. Surprisingly, there was also a subset of transcripts that was specifically up-regulated in *Mov10l1*$^{-/-}$ mice at P14. Among those, the most pro-

Fig. 4. MOV10L1 interacts with Piwi proteins and is necessary for piRNA-dependent repression of retrotransposons. (*A* and *B*) Up-regulation of retrotransposons in *Mov10l1*$^{-/-}$ mice. (*A*) Microarray analysis of pooled total RNA (*n* = 3) from testes of *Mov10l1*$^{-/-}$ mice versus *Mov10l1*$^{+/-}$ mice at postnatal days 10, 12, and 14. The depicted retrotransposon families from the LINE and LTR class were among the strongest up-regulated transcripts in *Mov10l1*$^{-/-}$ mice at P14. (*B*) Immunofluorescent staining of testis sections from P14 mice for the LINE ORF1 protein (ORF1p, green); counterstaining of nuclei with DAPI (blue). (*C*) Total RNA of testis from 24-d-old *Mov10l1*$^{+/-}$ mice versus *Mov10l1*$^{-/-}$ mice was end-labeled with [^{32}P]ATP and detected after denaturing PAGE. In *Mov10l1*$^{-/-}$ mice, ~29-nucleotide-long RNAs, most likely representing piRNAs, were strongly reduced. (*D*) Total RNA from testis of P14 and P24 *Mov10l1*$^{+/-}$ versus *Mov10l1*$^{-/-}$ mice was isolated and used for Northern blotting to detect specific piRNAs (piR-4868 and piR-1) and miRNAs (let-7a). An ethidium bromide-stained polyacrylamide gel is shown as a loading control. (*E*) Detection of the Piwi proteins Mili and Miwi (white) in testis sections from P14 *Mov10l1*$^{+/-}$ versus *Mov10l1*$^{-/-}$ mice by immunofluorescent staining. (*F*) COS1 cells were cotransfected with expression plasmids for Flag-tagged MOV10L1 and Myc-tagged MILI and MIWI, respectively. Lysates were then used for coimmunoprecipitation with anti-Flag antibodies followed by Western blot analysis with anti-Myc antibodies. Input lanes represent 1% of lysates used for coimmunoprecipitation. The experiment was repeated three times; representative immunoblots are shown. Reciprocal coimmunoprecipitation worked similarly.
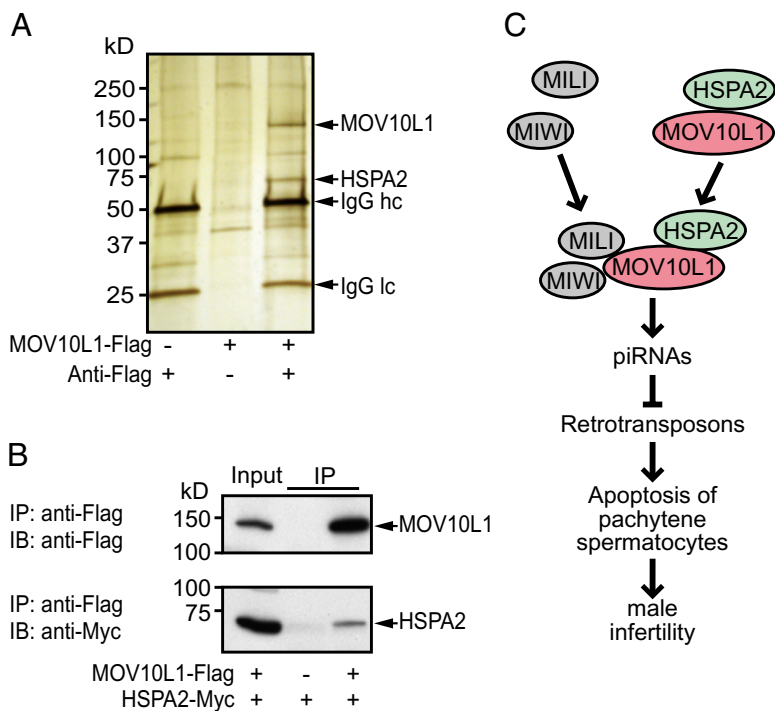
minent up-regulated transcripts represented retrotransposons from the LINE and LTR family, and up-regulation of some of those retrotransposons started as early as P10 (Fig. 4*A*).

We looked by immunostaining for expression of ORF 1 protein (ORF1p), one of the two proteins expressed by functional LINE retrotransposons, in testis sections of 14-d-old *Mov10l1*⁻/⁻ mice. Although there was nearly no ORF1p detectable in *Mov10l1*⁺/⁻ mice, more mature spermatocytes of nearly all seminiferous tubules of *Mov10l1*⁻/⁻ mice showed strong cytoplasmic and nuclear ORF1p expression (Fig. 4*B*).

Because it is known that piRNAs repress retrotransposon expression in testis, we determined small RNA expression in testes of *Mov10l1*⁻/⁻ mice by radioactive SDS-PAGE (Fig. 4*C*). Remarkably, expression of ~29-nucleotide RNAs, most likely representing piRNAs, was abolished in *Mov10l1*⁻/⁻ mice. Also, individual piR-NAs that were detected by Northern blot analysis were absent in *Mov10l1*⁻/⁻ mice (Fig. 4*D*, *Top*), which might be at least partially due to the loss of the piRNA-rich pachytene spermatocytes and later germ cells in *Mov10l1*⁻/⁻ mice. MOV10, the close homolog of MOV10L1, was recently identified as an interaction partner of Argonaute 1 and 2 in HeLa cells and suggested to be involved in microRNA processing (10). However, in *Mov10l1*⁻/⁻ mice, expression of microRNAs (e.g., let-7a) seemed to be unaffected (Fig. 4*D*, *Bottom*). This is not surprising, given that complete removal of microRNAs in germ cells by testis-specific deletion of Dicer 1 caused a severe reduction in the number of elongating spermatids and motile mature sperm (24), in contrast to deletion of *Mov10l1*.

MOV10L1 Interacts with the Piwi Proteins MIWI and MILI. Proper piRNA processing and function require a multiprotein complex that contains as core components members of the Piwi protein family. Piwi proteins represent a subfamily of Argonaute proteins containing a Piwi and a PAZ domain. Three PIWI protein homologs have been identified in the mouse genome: MIWI, MIWI2, and MILI. Genetic deletion of each Piwi protein results in male infertility; deletions of *Miwi2* and *Mili* block spermatogenesis at early prophase of meiosis I, and deletion of *Miwi* blocks post-meiotically in round spermatids (17–19). *Mov10l1* and *Mili* display

similar expression patterns, and deletion of *Mov10l1* in mice seems to phenocopy most closely the deletion of *Mili*.

We therefore analyzed expression of Piwi proteins in *Mov10l1*⁻/⁻ mice. *Miwi* and *Mili* mRNA expression was strongly induced in *Mov10l1*⁺/⁻ mice at P14, but was abrogated in *Mov10l1*⁻/⁻ mice (Fig. S4), possibly due to an arrest of spermatocyte differentiation before the onset of *Miwi*/*Mili* expression. To determine protein expression of MILI and MIWI, we performed immunofluorescent staining with specific antibodies on testis sections of 14-d-old mice. Protein expression of MIWI and MILI was undetectable in *Mov10l1*⁻/⁻ mice (Fig. 4*E*).

To investigate a possible direct interaction of MILI and MIWI with MOV10L1, we assayed whether MOV10L1 could coimmunoprecipitate with MILI or MIWI in COS cells. Indeed, both MILI and MIWI could directly bind to MOV10L1 (Fig. 4*F*).

Loss of MILI protein in spermatocytes of *Mov10l1*⁻/⁻ mice could explain the phenotype seen in *Mov10l1*⁻/⁻ mice. However, in contrast to the deletion of MOV10L1, deletion of MILI and other Piwi complex proteins such as MIWI2, GASZ, or Maelstrom results in a progressive loss of undifferentiated germ cells with age (19, 20, 22, 25). Nevertheless, because *Mov10l1* is already expressed at low levels in gonocytes, we cannot exclude the possibility that gonocytes of *Mov10l1*⁻/⁻ mice exhibit an altered methylation status of retrotransposon regions as seen in mice with deletion of *Miwi2*, which also have a block of spermatogenesis during meiosis even though *Miwi2* is expressed only before birth (19).

HSPA2 Is an Interaction Partner of *Mov10l1*. To identify other interaction partners of MOV10L1, we bound Flag-tagged MOV10L1 to IgG-Flag-Sepharose, incubated it with testis lysates from 20-d-old wild-type mice, and separated the coimmunoprecipitate by SDS-PAGE followed by silver staining (Fig. 5*A*). In addition to the MOV10L1 band, which migrated near its predicted molecular weight of 133 kDa, we identified a protein of ~70 kDa that was absent in the control lanes. Mass spectrometric (MS) analysis revealed that the 70-kDa band was heat shock 70-kDa protein 2 (HSPA2) (Fig. S5*A*). By performing a BLAST search with the individual peptide fragments that were identified in the 70-kDa band by MS,

we verified that HSPA2 originated from the mouse-testis lysate, not from the monkey-derived COS cells, in which we had generated the recombinant MOV10L1 protein (Fig. S5*B*). Interestingly, onset of *Hspa2* expression in pachytene spermatocytes coincides with the time when *Mov10l1* expression increases (Fig. S5*C*). Furthermore, genetic deletion of *Hspa2* in mice caused a phenotype remarkably similar to that of *Mov10ll*$^{-/-}$ mice (26). However, the mechanistic basis for the spermatogenic arrest in *Hspa2*$^{-/-}$ mice has been unclear. To confirm a direct interaction of HSPA2 with MOV10L1, we performed coimmunoprecipitation assays in COS cells and found that HSPA2 indeed binds directly to MOV10L1 (Fig. 5*B*).

HSPA2 belongs to the family of heat-shock proteins (HSPs), which are typically expressed upon sublethal heat shocks and other stresses. HSPA2, however, is constitutively expressed in brain and at higher levels in testis, where its expression starts with leptotene/zygotene spermatocytes (27). Low levels of *Hspa2* expression in humans were associated with low sperm count (oligozoospermia), suggesting that HSPA2 is necessary for sperm maturation or germ cell survival (28). HSPs often function as chaperones that stabilize the structure and facilitate the folding of other proteins. Our data, showing physical interaction between MOV10L1 and HSPA2, coupled with the similar phenotypes resulting from deletion of either gene, suggest that HSPA2 might be involved in MOV10L1 function, possibly by stabilizing MOV10L1.

Potential Clinical Relevance of MOV10L1. The fact that MOV10L1 does not seem to be necessary for germline stem-cell renewal suggests that the block of spermatogenesis in *Mov10l1*$^{-/-}$ mice might be reversible by reintroducing *Mov10l1* into germline stem cells. This might be clinically relevant if loss-of-function mutations in the *Mov10l1* gene are a cause for male infertility in humans. Furthermore, temporarily decreasing MOV10L1 expression (e.g., by siRNA or small molecules) or inhibiting MOV10L1 activity might be a reversible means for male birth control. This approach might also be relatively safe because full-length MOV10L1 seems to be expressed in males only in germ cells and loss of MOV10L1 in mice affected only spermatogenesis.

Finally, we note that *Mov10l1*, in addition to being expressed in the testis, is also expressed as a cardiac-specific isoform in the heart (9, 13). We have thus far observed no cardiac abnormalities in *Mov10l1*$^{-/-}$ mice. It will be interesting, however, to determine whether MOV10L1 plays a role in the heart under conditions of stress.

Materials and Methods

In Situ Hybridization. In situ hybridization was performed on paraformaldehyde (PFA)-fixed sections with probes directed against the 3′ UTR and, respectively, the C-terminal region of *Mov10l1*. ^{35}S-UTP–labeled sense and antisense RNA probes were generated by in vitro transcription with SP6 and T7 polymerase (Maxiscript, Ambion), respectively.

Immunohistological Examination. For immunofluorescence staining, PFA-fixed sections were deparaffinized and then boiled for 10 min in citrate solution (BioGenex) for antigen retrieval. After 30 min blocking with 2% goat serum, sections were incubated overnight at 4 °C with primary antibody. Anti-rabbit antibodies conjugated with Alexa 488 (1:500; Invitrogen) were used as secondary antibodies.

Coimmunoprecipitation. COS cells were transfected with pCMV6 expression vectors for N-terminal Flag-tagged MOV10L1 and N-terminal Myc-tagged MIWI, MILI, and HSPA2, respectively. After 48 h, COS cells were lysed in 10 mM Tris–HCl pH 7.4 buffer containing 150 mM NaCl, 0.1% Triton X-100 and protease inhibitors (complete mini; Roche). After syringe-and-needle homogenization, the cell lysate was centrifuged 10 min at $15,000 \times g$. The supernatant was then preincubated for 2 h with Protein A/G Sepharose (Ultralink, Pierce). Immunoprecipitation was carried out with mouse anti-FLAG M2 antibody (#F1804, Sigma). Immunoprecipitates were then separated by 10% gradient SDS-PAGE (Bio-Rad) and analyzed by Western blotting using mouse anti-Myc antibody (1:2,000, #sc-40, Santa Cruz Biotechnology).

Generation of Conditional *Mov10l1* Knockout Mice. For generation of the *Mov10l1* targeting vector, the pGKNEO-F2L2DTA plasmid (Addgene plasmid 13445) was used. All experimental animal procedures were approved by the Institutional Animal Care and Research Advisory Committee at the University of Texas Southwestern Medical Center. Experiments are described in more detail in *SI Materials and Methods*.

1. Cordaux R, Batzer MA (2009) The impact of retrotransposons on human genome evolution. *Nat Rev Genet* 10:691–703.
2. Babushok DV, Kazazian HH, Jr (2007) Progress in understanding the biology of the human mutagen LINE-1. *Hum Mutat* 28:527–539.
3. Brouha B, et al. (2003) Hot L1s account for the bulk of retrotransposition in the human population. *Proc Natl Acad Sci USA* 100:5280–5285.
4. Kazazian HH, Jr (2004) Mobile elements: Drivers of genome evolution. *Science* 303:1626–1632.
5. Aravin AA, Bourc'his D (2008) Small RNA guides for de novo DNA methylation in mammalian germ cells. *Genes Dev* 22:970–975.
6. Ahmed EA, de Rooij DG (2009) Staging of mouse seminiferous tubule cross-sections. *Methods Mol Biol* 558:263–277.
7. Aravin AA, Hannon GJ (2008) Small RNA silencing pathways in germ and stem cells. *Cold Spring Harb Symp Quant Biol* 73:283–290.
8. Girard A, Sachidanandam R, Hannon GJ, Carmell MA (2006) A germline-specific class of small RNAs binds mammalian Piwi proteins. *Nature* 442:199–202.
9. Liu ZP, et al. (2001) CHAMP, a novel cardiac-specific helicase regulated by MEF2C. *Dev Biol* 234:497–509.
10. Meister G, et al. (2005) Identification of novel argonaute-associated proteins. *Curr Biol* 15:2149–2155.
11. Malone CD, et al. (2009) Specialized piRNA pathways act in germline and somatic tissues of the Drosophila ovary. *Cell* 137:522–535.
12. Vagin VV, et al. (2006) A distinct small RNA pathway silences selfish genetic elements in the germline. *Science* 313:320–324.
13. Ueyama T, Kasahara H, Ishiwata T, Yamasaki N, Izumo S (2003) Csm, a cardiac-specific isoform of the RNA helicase Mov10l1, is regulated by Nkx2.5 in embryonic heart. *J Biol Chem* 278:28750–28757.
14. Wang PJ, McCarrey JR, Yang F, Page DC (2001) An abundance of X-linked genes expressed in spermatogonia. *Nat Genet* 27:422–426.
15. Liu ZP, Olson EN (2002) Suppression of proliferation and cardiomyocyte hypertrophy by CHAMP, a cardiac-specific RNA helicase. *Proc Natl Acad Sci USA* 99:2043–2048.
16. Lovasco LA, et al. (2010) Accelerated ovarian aging in the absence of the transcription regulator TAF4B in mice. *Biol Reprod* 82:23–34.
17. Deng W, Lin H (2002) miwi, a murine homolog of piwi, encodes a cytoplasmic protein essential for spermatogenesis. *Dev Cell* 2:819–830.
18. Kuramochi-Miyagawa S, et al. (2004) Mili, a mammalian member of piwi family gene, is essential for spermatogenesis. *Development* 131:839–849.
19. Carmell MA, et al. (2007) MIWI2 is essential for spermatogenesis and repression of transposons in the mouse male germline. *Dev Cell* 12:503–514.
20. Ma L, et al. (2009) GASZ is essential for male meiosis and suppression of retrotransposon expression in the male germline. *PLoS Genet* 5:e1000635.
21. Shoji M, et al. (2009) The TDRD9-MIWI2 complex is essential for piRNA-mediated retrotransposon silencing in the mouse male germline. *Dev Cell* 17:775–787.
22. Unhavaithaya Y, et al. (2009) MILI, a PIWI-interacting RNA-binding protein, is required for germ line stem cell self-renewal and appears to positively regulate translation. *J Biol Chem* 284:6507–6519.
23. Buaas FW, et al. (2004) Plzf is required in adult male germ cells for stem cell self-renewal. *Nat Genet* 36:647–652.
24. Maatouk DM, Loveland KL, McManus MT, Moore K, Harfe BD (2008) Dicer1 is required for differentiation of the mouse male germline. *Biol Reprod* 79:696–703.
25. Soper SF, et al. (2008) Mouse maelstrom, a component of nuage, is essential for spermatogenesis and transposon repression in meiosis. *Dev Cell* 15:285–297.
26. Dix DJ, et al. (1996) Targeted gene disruption of Hsp70-2 results in failed meiosis, germ cell apoptosis, and male infertility. *Proc Natl Acad Sci USA* 93:3264–3268.
27. Inselman AL, et al. (2010) Heat shock protein 2 promoter drives cre expression in spermatocytes of transgenic mice. *Genesis* 48:114–120.
28. Cedenho AP, et al. (2006) Oligozoospermia and heat-shock protein expression in ejaculated spermatozoa. *Hum Reprod* 21:1791–1794.